Thin Solid Films 595 (2015) 221–225

Contents lists available at ScienceDirect

Thin Solid Films

journal homepage: www.elsevier.com/locate/tsf

Blue to red emission from as-deposited nc-silicon/silicon dioxide by hot wire chemical vapor deposition

A. Dutt [a], Y. Matsumoto [a,*], J. Santoyo-Salazar [b], G. Santana-Rodríguez [c], S. Godavarthi [d]

[a] SEES, Electrical Engineering Department, Centro de Investigación y de Estudios Avanzados del IPN, México City 07360, Mexico
[b] Departamento de Física, Centro de Investigación y de Estudios Avanzados del IPN, México City 07360, Mexico
[c] Instituto de Investigaciones en Materiales, Universidad Nacional Autónoma de México, Coyoacán, México City 04510, Mexico
[d] Instituto de Ciencias Físicas, Universidad Nacional Autónoma de México, Cuernavaca City, Morelos 62210, Mexico

ARTICLE INFO

Article history:
Received 30 January 2015
Received in revised form 28 May 2015
Accepted 28 May 2015
Available online 30 May 2015

Keywords:
Nanocrystalline Silicon / Nanocrystalline Silicon Dioxide
White Bright Photoluminescence
Hot-wire chemical vapor deposition
Tungsten wire

ABSTRACT

Silicon thin films have been obtained with respect to the deposition time variation by using hot wire chemical vapor deposition. Silicon and related oxide particles both in crystalline phases embedded in amorphous silicon have been obtained by using tungsten as the catalyst material for the decomposition of source gases in the reaction chamber. Crystalline nature of the thin film has been shown using X-ray diffraction, transmission electron microscopy and scanning electron microcopy. X-ray diffraction patterns authenticate the presence of crystalline phases related to silicon and silicon dioxide in the matrix. Furthermore, transmission electron micrographs also revealed the presence of adjacent nature of silicon and silicon dioxide particles in the amorphous matrix. The as-deposited samples at low substrate temperature of about 200 °C have shown intense white photoluminescence spectra. No need of post-deposition annealing for light emission at room temperature has been demonstrated. This advantage of hot wire chemical vapor deposition technique could be considered for the mass production of optoelectronic devices in the future.

1. Introduction

Several investigations are being carried out for improving the film quality of silicon based thin films and to produce optoelectronic devices based on Si nanocrystals or quantum dots [1–5]. However, it is still necessary to understand the mechanism for optical emission from these small nano-particles and to attain visible emission. For this reason, many groups have been depositing silicon quantum dots in various oxide or nitride matrixes to achieve effective confinement [6–12] and hence, demonstrate the size dependent luminescence. Until now, silicon thin films have been deposited and used widely to fabricate efficient solar cells [13–15] but still the remaining part is to explore further potential of this material for optoelectronic applications. Not enough information related to morphology, size and photoluminescence (PL) correlations are the main causes of the limited optical-device fabrication development.

Hot wire chemical vapor deposition (HW-CVD) is a special technique in itself due to the unique principle of operation of using heated (thermal catalytic reaction) filament for the decomposition of gases which allows the formation of nano-crystallites easily without adding any complexity to the process [16,17]. Apart from this, it offers some other benefits like efficient use of source gases and no plasma damage on the depositing thin films. Earlier, other groups have reported different deposition conditions; for instance, filament temperature, deposition pressure and substrate to filament distance to improve the film quality [18–20]. Process pressure determines the species concentration available in the chamber for film growth, whereas filament temperature and its distance to sample substrate determine how effectively sources gases are being decomposed and diffused on. Even one of the recent reports mentioned the formation of silicon nano-crystallites using HW-CVD without the need of annealing, but, however for achieving PL response the samples have to be heated at the elevated temperatures in N_2 atmosphere [21].

In this article, by the variation of deposition time it has been controlled the crystalline-sizes in the a-SiO_x matrix. Thin films obtained at low substrate temperature shows the nano-particles related to the silicon and silicon dioxide which have been observed by X-ray diffraction (XRD) and transmission electron microscopy (TEM). Visible photoluminescence emissions from as-deposited samples were observed at room temperature without any post-deposition annealing treatments.

2. Sample preparation and characterization technique

HW-CVD system used for the deposition consists of a stainless-steel chamber evacuated through a turbo molecular pump (Varian model V-550) as has been described elsewhere [16,22]. The initial chamber

* Corresponding author.
E-mail address: ymatsumo@cinvestav.mx (Y. Matsumoto).

http://dx.doi.org/10.1016/j.tsf.2015.05.061
0040-6090/

background pressure was maintained at 1.3×10^{-4} Pa. Source gases were directed towards a tungsten (W) 0.75 mm diameter wire and the distance between the filament and substrate was kept constant at 5 cm. The filament temperature (T_{fil}) was settled at 1800 °C while the substrate temperature (T_{subs}) was 200 °C. The gas flow rates were maintained at 5 sccm (standard cubic centimeter per minute) for both pure silane (SiH_4) and hydrogen (H_2). 10% of diborane (B_2H_6) diluted in hydrogen was maintained at 10 sccm and oxygen (O_2) at 0.5 sccm for 20 min. The above flow rates of the gases viz. ($SiH_4/H_2/B_2H_6/O_2 = 5/5/10/0.5$) were maintained constant for all of the depositions described in the text. After allowing the flow of all four gases, the pressure in the chamber was maintained at 13.33 Pa using a throttle valve (Baratron, model-253B-20-40-2), from MKS Instruments Corporate (Six Shattuck Road, Andover, MA, USA). Transitions among phases were analyzed by X-ray diffraction, XRD-Siemens model D5000 configured with Cu-K-alpha radiation ($\lambda = 1.5418$ Å) generated at 25 mA and 35 kV. Diffraction patterns were obtained at (θ–2θ) configuration from 20–80° (2θ) by using a step of 0.02° every 10 s, and the transmittance spectra were measured by Shimadzu UV-2401PC. Photoluminescence (PL) spectra were obtained using a Kimmon Koha He–Cd laser with an excitation wavelength of 325 nm and bright field images were obtained in a transmission electron microscope, TEM (JEOL-JEM-2010) at 200 kV with a wavelength, $\lambda = 0.027$ Å, and camera distance, L = 20 cm. Sample preparation for TEM was done by scraping the surface of thin films. The fragments of samples were supported by dispersion in Cu-grids—400 mesh with formvar carbon layer. A Field Emission Scanning Electron Microscope, FESEM-Carl Zeiss-AURIGA was used to capture the morphological related micrographs at 2.0 kV.

3. Results and discussions

3.1. XRD analysis of nc-Si/nc-SiO_2 in SiO_x films

Fig. 1 shows the XRD pattern of the as-deposited samples for the indicated deposition times. From the pattern, two notable features could be observed. Firstly, the broad XRD peaks determine the presence of small sized nano-particles, and finally, the peaks at 25.4 and 42.4° show the presence of SiO_2 phase along with the three well-known peaks for Si at 28.4, 47.4 and 56.1° corresponding to (111), (220) and (311), respectively. Also, the peak tendencies confirm that the deposited films are polycrystalline in nature. The effect of deposition time and hence thickness was evaluated with the change in the intensities of the X-ray diffraction patterns rather than movement in peaks. Increase in intensity of the thin film with the increase in deposition time could be explained by the increase in size of small crystallites. The appearance of two other detected peaks at 25.4 and 42.4° corresponds to (533) and (200) silicon dioxide phases, respectively [23,24]. In the later Section 3.3, more analysis has been done to confirm this assumption.

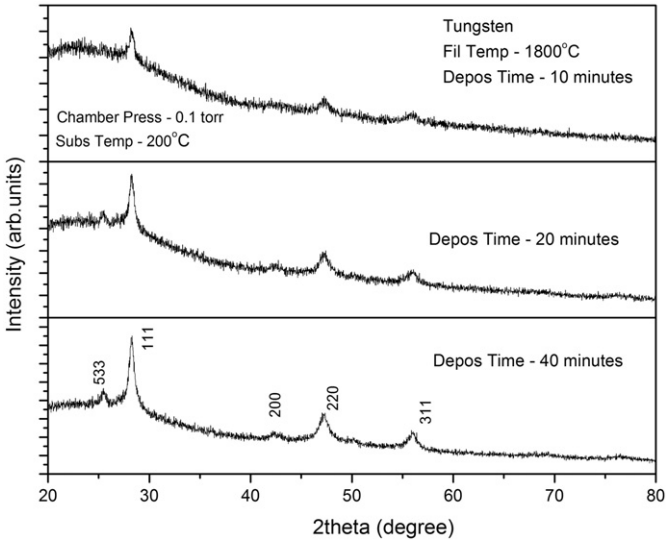

Fig. 1. XRD patterns of as-deposited samples deposited for 10, 20, and 40 min.

3.2. UV–vis spectroscopy analysis

The optical absorption spectra of the Si thin film samples were recorded in the range of 250 nm to 1100 nm. From Fig. 2(A) it could be observed for lower deposition time that the absorption edge appears in the lower wavelength (or higher energies) region which remarks the broadening of band gap whereas contrary effect has been found for the other samples. Optical-band gap was estimated from transmittance data using Swanepoel's procedure [25]. Fig. 2(B) shows the calculated optical band gap and the thickness for three deposited samples. Decrease in band gap could be seen with the increase in the deposition time whereas thickness effect is divergent to band gap. Three different thicknesses corresponding to the different deposition times (10, 20 and 40 min) were found to be 307, 540 and 855 nm, respectively.

3.3. Scanning electron microscopy (SEM), transmission electron microscopy (TEM) and PL analysis

For detailed morphological analysis and estimation of possible structure of nano-particles, SEM studies have been carried out. The images in

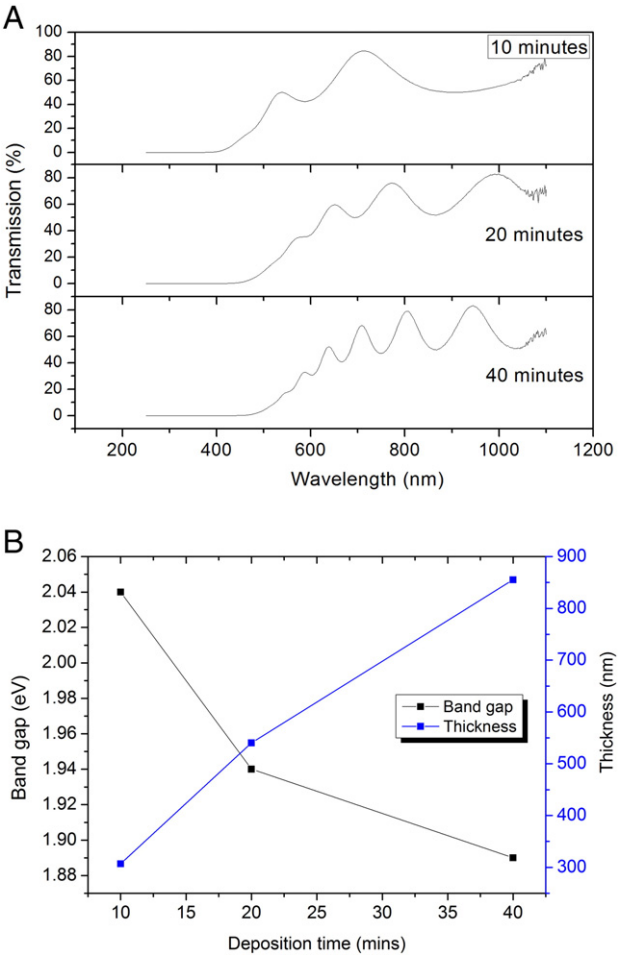

Fig. 2. (A) UV–vis spectra and (B) optical band gap and as-deposited sample thickness as a function of deposition time.

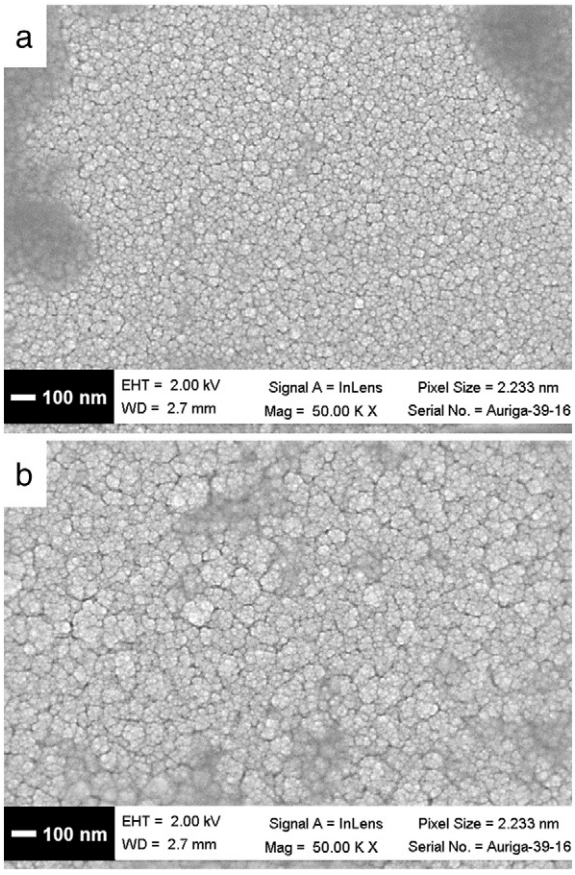

Fig. 3. SEM images of samples: (a) 20 min and (b) 40 min.

Fig. 3(a) and (b) exhibited that the grains are smooth and homogenous in their respective morphology. However, increase in the size of grains could be found for the sample deposited at 40 min of deposition time as compared to the other samples deposited at 20 min.

To understand the presence of the crystalline structure and particle sizes, TEM studies have been made. Fig. 4(a) and (b) shows the plane view bright field image of sample deposited at 20 min of deposition. Fig. 4(c) shows the TEM analysis for one of the selected areas as shown in Fig. 4(b). It could be observed that the particle structure is like agglomeration of different planar orientations. Fig. 4(d) shows the interatomic distances of silicon related planes. However, from Fig. 4(c), some crystal orientations corresponding to SiO_2 plane dispersed in the amorphous matrix could be observed. These planes were found by the crystalline contributions (111) at 3.10 Å, (200) at 2.17 Å and (311) at 1.70 Å in the nanoparticles and also confirm the observations made by the XRD analysis. The selected area electron diffraction, SAED (Fig. 4(e)) was taken at global area presented in Fig. 4(b). These diffraction rings correspond to the crystalline planes obtained with XRD in Fig. 1. The SAED versus XRD analysis indicates that the plane (200) had a low intensity due to the crystal contributions of these planes from the nanoparticles. Like the structure and morphology, PL response also greatly depends on the deposition conditions. Fig. 5 corresponds to the PL spectra of as-grown samples. PL was measured using a He–Cd laser at the ambient temperature. From the spectra it could be observed as the deposition time, the film thickness increases provoking a shift for PL spectra.

3.4. Discussion

According to the theoretical concepts associated with the quantum confinement, PL in the visible region can only be obtained from silicon nano-clusters no more than 4.9 nm in its diameters. However, explaining the exact nature of mechanism from silicon thin films is always a difficult task due to the close presence of the energy levels due to the size of the nano-particles as well as the various known defect sites for this material.

In the present case, there are two important parameters which have to be considered: firstly, the broad visible PL peak from all of the samples and secondly, the shift in the peak for three respective samples.

Broad PL peak could be assigned as the contribution of combined effects of the trap levels or the energy distribution associated with the various defect sites or also it could be due to the energy levels of different sizes of the nano-particles in the matrix observed in the TEM image

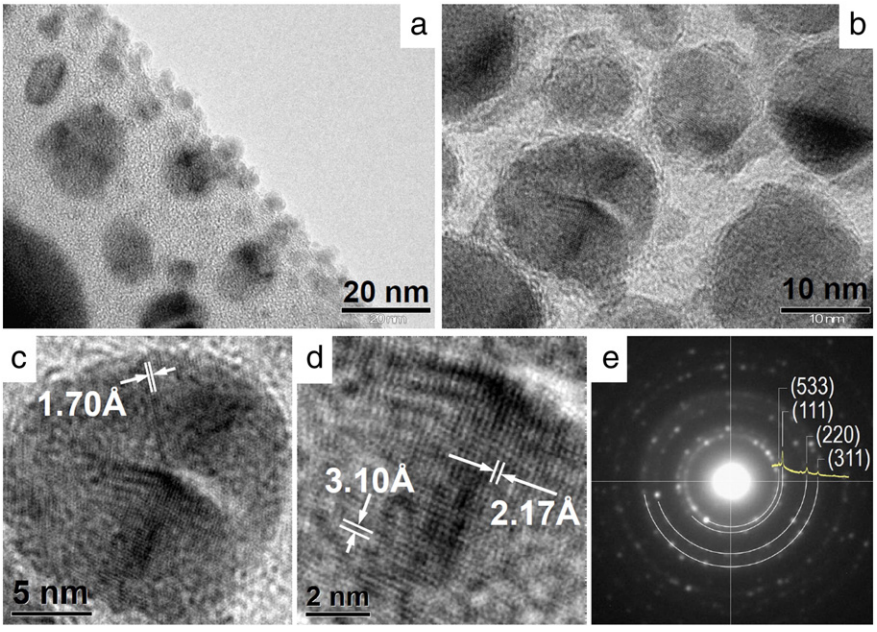

Fig. 4. TEM images at different magnification of as-deposited sample (deposition time: 20 min): (a) and (b) global distribution, (c) different crystal contributions in a particle, (d) crystalline planes, and (e) SAED versus XRD pattern.

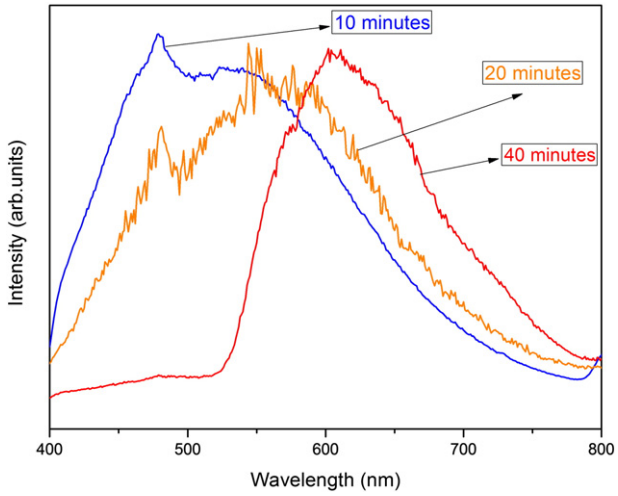

Fig. 5. Room temperature PL for W-filament deposited samples with respect to deposition time.

in Fig. 4(a). Defect sites could give rise to a broad PL response which could be assigned to the combined contribution of red (1.96 eV), green (2.3 eV) and blue (2.8 eV) bands. Non-bridging oxygen hole center (NBOHC) generally gives rise to the red band [26] whereas, the presence of green band has been attributed to hydrogen-bonding related species in the thin film with composites of SiO_2 nano-particles [27]. Even surface trapped excitons (STE) give rise to wide range luminescence spectra between 2 and 3 eV [28].

There exists a well-known relation between the size of the particles and the luminescence band gap [29]:

$$Epl = Eg + \frac{3.73}{d^{1.39}}.$$

Obtained band gap from this relation for the deposited samples is found to be in the range of 1.7 to 2.5 eV and also matches with the band gap calculated in Fig. 2(B) which determines the distribution of nanoparticle in the range of 3–4 nm in the matrix. It interferes that the excited exciton pairs have the possibility to get trapped either in the energy levels due to the defect sites or existing levels due to the size of particles. However, if confinement has the solitary role in the wide visible spectra, there has to be a complete homogenous nature of the deposited film and the size distribution has to be in the region of <4.9 nm. Controlling that level of homogenous nature in chemical vapor deposition technique is still a difficult task to achieve. In that case there is a huge probability of the presence of wide distribution of nanoparticles of various sizes along with the defects which could be also held responsible for visible emission. Additionally, shift in the PL spectra could be either due to the confinement of excitons due to the size of particles [30] or the effect of interference due to the absorption phenomenon [31]. In the present study, PL peak intensity has been normalized for three respective samples to make clear the mechanism of emission and from Figs. 3 and 5, shift observed for the three samples remarks the strong possibility of emission due to the trapping of excitons in energy levels due to the smaller size of particles. Specially, the SEM image clarifies the morphology in Fig. 3 and shows the variation in size of grains along with the thickness for different conditions.

Moreover as we observed from Figs. 1 and 4(c) samples not only have crystalline silicon phases but also there is presence of the silicon dioxide crystalline phases. The presence of silicon dioxide crystalline phases at this low temperature without post-annealing treatments shows the prominence of this material as it could create a well passivated structure without remaining dangling bonds [10]. This kind of material could be helpful in the future for various applications including electronics and biomedical areas.

4. Conclusions

It has been obtained stable silicon and silicon oxide nano-particles at low temperature of 200 °C by means of HW-CVD. The presence of smaller sized particles which are well passivated by oxygen bonding has shown intense visible emission at room temperature without any means of post-deposition heat treatment. This kind of low temperature deposited material using HW-CVD could open an outlook for further noble device fabrication. However, at the same time, one cannot neglect the close presence of various defect sites which could also play role in an optical emission along with the nanoparticles.

Acknowledgments

The authors thank Angela Gabriela López for the sample preparations. The authors are indebted to Marcela Guerrero for the technical assistance. We would express our sincere thanks to Josué E. Romero-Ibarra for the SEM measurements. This project is supported by the National Council of Science and Technology (CONACYT) Nos. CB2009-128723 and CB2012-179632.

References

[1] T. Makimura, Y. Yamamoto, S. Mitani, T. Mizuta, C.Q. Li, D. Takeuchi, K. Murakami, Phosphorus-doped Si nanocrystallites embedded in SiO_2 films, Appl. Surf. Sci. 197–198 (2002) 670.
[2] L. Khomenkova, N. Korsunska, T. Torchynska, Y. Yokhimchuk, B. Jumayev, A. Many, Y. Goldstein, E. Savir, J. Jedrzejewski, Defect-related luminescence of Si/SiO_2 layers, J. Phys. Condens. Matter 14 (2002) 13217.
[3] M. Nayfeh, S. Rao, N. Barry, J. Therrien, G. Belomoin, A. Smith, S. Chaieb, Observation of laser oscillation in aggregates of ultrasmall silicon nanoparticles, Appl. Phys. Lett. 80 (2002) 121.
[4] L. Pavesi, L. Dal Negro, C. Mazzoleni, G. Franzò, F. Priolo, Optical gain in silicon nanocrystals, Nature 480 (2000) 440.
[5] P.M. Fauchet, L. Tsybeskov, S.P. Duttagupta, K.D. Hirschman, Stable photoluminescence and electroluminescence from porous silicon, Thin Solid Films 297 (1997) 254.
[6] M.S. Yang, K.S. Cho, J.H. Jhe, S.Y. Seo, J.H. Shin, K.J. Kim, D.W. Moon, Effect of nitride passivation on the visible photoluminescence from Si-nanocrystals, Appl. Phys. Lett. 85 (2004) 3408.
[7] R. Smirani, F. Martin, G. Abel, Y.Q. Wang, M. Chicoine, G.G. Ross, The effect of size and depth profile of Si-nc imbedded in a SiO_2 layer on the photoluminescence spectra, J. Lumin. 115 (2005) 62.
[8] Z.T. Kang, B. Arnold, C.J. Summers, B.K. Wagner, Synthesis of silicon quantum dot buried SiO_x films with controlled luminescent properties for solid-state lighting, Nanotechnology 17 (2006) 4477.
[9] T.W. Kim, C.H. Cho, B.H. Kim, S.J. Park, Quantum confinement effect in crystalline silicon quantum dots in silicon nitride grown using SiH_4 and NH_3, Appl. Phys. Lett. 88 (2006) 123102.
[10] M.V. Wolkin, J. Jorne, P.M. Fauchet, G. Allan, C. Delerue, Electronic states and luminescence in porous silicon quantum dots: the role of oxygen, Phys. Rev. Lett. 82 (1999) 197.
[11] G. Santana, B.M. Monroy, A. Ortiz, L. Huerta, J.C. Alonso, J. Fandiño, J. Aguilar-Hernández, E. Hoyos, F. Cruz-Gandarilla, G. Contreras-Puentes, Influence of the surrounding host in obtaining tunable and strong visible photoluminescence from silicon nanoparticles, Appl. Phys. Lett. 88 (2006) 041916.
[12] A. Dutt, Y. Matsumoto, S. Godavarthi, G. Santana-Rodríguez, J. Santoyo-Salazar, A. Escobosa, White bright luminescence at room temperature from TEOS-based thin films via catalytic chemical vapor deposition, Mater. Lett. 131 (2014) 295.
[13] S. Klein, M. Rohde, S. Buschbaum, D. Severin, Throughput optimized a-Si/μc-Si tandem solar cells on sputter-etched ZnO substrates, Sol. Energy Mater. Sol. Cells 98 (2012) 363.
[14] W. Hoffmann, T. Pellkofer, Thin films in photovoltaics: technologies and perspectives, Thin Solid Films 520 (2012) 4094.
[15] Y. Matsumoto, M. Ortega, F. Wiinsch, Z. Yu, Cat-CVD deposited inverted μc-Si:H/c-Si heterojunction solar cell approach, 5th International Conference on Electrical Engineering, Computing Science and Automatic Control (CCE 2008) 2008, p. 455.
[16] Y. Matsumoto, S. Godavarthi, M. Ortega, V. Sánchez, S. Velumani, P.S. Mallick, Size modulation of nanocrystalline silicon embedded in amorphous silicon oxide by Cat-CVD, Thin Solid Films 519 (2011) 4498.
[17] A. Coyopol, G. García-Salgado, T. Díaz-Becerril, H. Juárez, E. Rosendo, R. López, M. Pacio, J.A. Luna-López, J. Carrillo-López, Optical and structural properties of silicon nanocrystals embedded in SiO_x matrix obtained by HWCVD, J. Nanomater. 2012 (2012) 368268.

[18] H.L. Duan, G.A. Zaharias, Stacey F. Bent, The effect of filament temperature on the gaseous radicals in the hot wire decomposition of silane, Thin Solid Films 395 (2001) 36.
[19] S.R. Jadkar, J.V. Sali, S.T. Kshirsagar, M.G. Takwale, Influence of process pressure on HW-CVD deposited a-Si:H films, Sol. Energy Mater. Sol. Cells 85 (2005) 301.
[20] S.K. Chong, B.T. Goh, C.F. Dee, S.A. Rahman, Effect of substrate to filament distance on formation and photoluminescence properties of indium catalyzed silicon nanowires using hot-wire chemical vapor deposition, Thin Solid Films 529 (2013) 153.
[21] A. Coyopol, T. Díaz-Becerril, G. García-Salgado, H. Juárez-Santisteban, R. López, E. Rosendo-Andrés, Evolution on the structural and optical properties of SiO_x films annealed in nitrogen atmosphere, J. Lumin. 145 (2014) 88.
[22] Y. Matsumoto, Hot wire-CVD deposited a-SiO_x and its characterization, Thin Solid Films 501 (2006) 95.
[23] H.E. Swanson, R.K. Fuyat, Supplementary list of publications of the National Bureau of Standards July 1, 1947 to June 30, 1957, Natl. Bur. Stan. (U.S.) Circ. 539 (1953) 3.
[24] V. Fülop, G. Borbely, H.K. Beyer, S. Ernst, J. Weitkamp, J. Chem. Soc. Faraday Trans. 1 (85) (1989) 2127.
[25] R. Swanepoel, Determination of the thickness and optical constants of amorphous silicon, J. Phys. E Sci. Instrum. 16 (1983) 1214.
[26] G. Pacchioni, L. Skuja, D.L. Griscom, Defects in SiO_2 and related dielectrics, Sci. Technol. 2 (2000) 73.
[27] Yu.D. Glinka, S.H. Lin, Y.-T. Chen, The Photoluminescence from hydrogen-related species in composites of SiO_2 nanoparticles, Appl. Phys. Lett. 75 (1999) 778.
[28] C. Itoh, K. Tanimura, N. Itoh, Optical studies of self-trapped excitons in SiO_2, J. Phys. C Solid State Phys. 21 (1988) 4693.
[29] C. Delerue, G. Allan, M. Lannoo, Theoretical aspects of the luminescence of porous silicon, Phys. Rev. B 48 (1993) 11024.
[30] W.D.A.M. de Boer, D. Timmerman, K. Dohnalova, I.N. Yassievich, H. Zhang, W.J. Buma, T. Gregorkiewicz, Red spectral shift and enhanced quantum efficiency in phonon-free photoluminescence from silicon nanocrystals, Nat. Nanotechnol. 5 (2010) 878.
[31] A. Rodriguez-Gomez, A. Garcıa-Valenzuela, E. Haro-Poniatowski, J.C. Alonso-Huitron1, Effect of thickness on the photoluminescence of silicon quantum dots embedded in silicon nitride films, J. Appl. Phys. 113 (2013) (233102-1).